



Input and cycling of iron in the Gulf of Aqaba, Red Sea

Zanna Chase,¹ Adina Paytan,² Kenneth S. Johnson,³ Joseph Street,² and Ying Chen²

Received 24 October 2005; revised 5 April 2006; accepted 26 May 2006; published 1 September 2006.

[1] The Gulf of Aqaba, northern Red Sea, is an ideal natural laboratory for studying the impact of atmospheric dry deposition of iron to the ocean surface. We have measured atmospheric iron deposition weekly for 18 months, and dissolved and total dissolvable iron concentrations in the stratified summer (August) and well-mixed winter (March) water column. Concentrations of dissolved and total dissolvable iron remain roughly constant with depth in March. In August, there is a strong surface enrichment of iron. The accumulation of iron at the surface during the rain-free summer can be simulated by a one-dimensional model including atmospheric iron flux and estimates of iron scavenging, biological uptake and dissolution. An overall dissolution of 2% of dry deposited aerosol iron produces the best fit to the observations. A residence time of half a year for dissolved iron in surface waters with respect to scavenging is calculated for this region.

Citation: Chase, Z., A. Paytan, K. S. Johnson, J. Street, and Y. Chen (2006), Input and cycling of iron in the Gulf of Aqaba, Red Sea, *Global Biogeochem. Cycles*, 20, GB3017, doi:10.1029/2005GB002646.

1. Introduction

[2] The deposition and partial dissolution of mineral dust represents a major source of many bioactive trace metals and nutrients to the ocean. Iron has received the most attention because in many remote regions of the ocean dust deposition represents the major input of this important micronutrient [Duce and Tindale, 1991; Fung *et al.*, 2000; Moore *et al.*, 2002]. The atmospheric deposition rate of iron to the ocean surface varies over three orders of magnitude, from minimum values in the remote Pacific and Southern Ocean to maximum values near desert source regions [Duce and Tindale, 1991; Fung *et al.*, 2000].

[3] The total deposition of iron consists of wet and dry deposition. Recent work suggests precipitation scavenging may be responsible for as much as 30% of total iron deposition to the ocean [Gao *et al.*, 2003]. The fraction of iron that dissolves in both wet and dry deposition is conventionally referred to as the solubility, a term we retain here for consistency with the literature. This solubility is poorly constrained. These values are critical to understanding the biogeochemical fate of iron that falls on the surface of the ocean. For example, a recent model of iron supply and demand in the upper ocean [Moore *et al.*, 2002] found that using a global value of 2% solubility, small phytoplankton growth in 50% of the world ocean would be

limited by iron, whereas if solubility is 10%, small phytoplankton growth is limited by iron in only 26% of the ocean.

[4] The Gulf of Aqaba, Red Sea, is an ideal natural laboratory in which to study the process of atmospheric iron deposition to the ocean. The dust inputs are high, other inputs are minimal, and the system is oligotrophic and presumably not limited by iron, all factors that maximize the signal of aeolian deposition in the ocean.

[5] The Gulf of Aqaba is the northeastern extension of the Red Sea, bordered by Israel, Jordan, Egypt and Saudi Arabia. It is a deep, narrow, semienclosed basin surrounded by desert. The Gulf receives large dust inputs from the Sahara and adjacent deserts. Precipitation and runoff are close to zero and benthic sources of iron are minimized by the steep shelf and intense summertime stratification. Exchange of seawater between the Gulf and the Red Sea proper occurs only across a 250-m sill at the southern end (the Straights of Tiran). During the summer the Gulf is thermally stratified, with mixed layer depths of about 20 m. Cooling in winter breaks down stratification and deep overturning occurs between November and April. Winter mixing can reach depths as great as 860 m during exceptionally cold winters [Genin *et al.*, 1995], though typically convective mixing reaches depths of 300–400 m. The Gulf is oligotrophic, with maximum chlorophyll *a* concentrations of ~ 0.75 mg m⁻³ in spring at the onset of stratification and minimum concentrations of ~ 0.25 mg m⁻³ in midsummer [Labiosa *et al.*, 2003]. The majority of the phytoplankton species are ultraphytoplankton (< 8 μ m). The cyanobacteria, *Synechococcus* and *Prochlorococcus*, dominate in the spring and summer, respectively, and eucaryotic species are more abundant during winter mixing [Lindell and Post, 1995]. *Trichodesmium* spp have been observed in the Gulf, and in some years contribute up to 35% of the primary productivity at the surface [Post *et al.*, 2002]. However, colony abundance is not as great as observed in other

¹College of Oceanic and Atmospheric Sciences, Oregon State University, Corvallis, Oregon, USA.

²Department of Geological and Environmental Sciences, Stanford University, Stanford, California, USA.

³Monterey Bay Aquarium Research Institute, Moss Landing, California, USA.

oligotrophic seas, such as the Caribbean and Sargasso and *Trichodesmium* spp are not observed every year and at all seasons [Post *et al.*, 2002].

[6] Given that the Gulf of Aqaba is a semi-enclosed basin surrounded by desert, we expected a priori that iron supply from atmospheric deposition would be sufficient to meet the demands of the phytoplankton community, including the nitrogen-fixing species. Iron-replete regions of the ocean are generally phosphorous-limited [Wu *et al.*, 2000], and the low concentrations of soluble reactive phosphorous in the Gulf ($0.003\text{--}0.07\ \mu\text{mol L}^{-1}$ in surface waters, Israeli National Monitoring of the Gulf of Eilat, www.iui-eilat.ac.il, and this work) would suggest this system is also phosphorous-limited. However, the Gulf of Aqaba lacks continental shelf in the traditional sense, and receives virtually no runoff, both factors that could limit the supply of nonatmospheric iron. It is also possible that the solubility of the aerosol iron deposited in the Gulf is anomalously low, owing to a combination of short atmospheric residence times and little wet deposition. To our knowledge dissolved iron had never been measured in the Gulf of Aqaba, so the true iron status of this area was not known. More broadly, we have combined a time series of aerosol measurements with water column measurements of dissolved and dissolvable iron in order to better understand the input and cycling of iron in an oligotrophic system with large inputs of iron by dry deposition.

2. Methods

2.1. Water Sample Collection

[7] Samples were collected from the Israeli side of the Gulf on 19–20 August 2003 and from both the Israeli and the Jordanian sides on 22–25 March 2004. Samples for iron were collected from a small fiberglass boat using all-plastic 5L GO-Flo bottles deployed on non-metallic line. The GO-Flo bottles were cleaned prior to deployment by soaking them in 1% hydrochloric acid and rinsing with ultra pure water and then with sample water. In August 2003 all samples were collected using the GO-Flos. In March 2004 surface samples were collected through acid-cleaned plastic tubing (C-flex) using a peristaltic pump. Immediately after collection, samples for dissolved iron were filtered from the GO-Flo bottles through in-line acid-cleaned $0.2\text{-}\mu\text{m}$ capsule filters with Supor membrane (Pall acropak). In August the filtration was driven by filtered, compressed air, and in March a peristaltic pump was used. Samples were collected in acid cleaned (1 day in dilute micro detergent, at least 1 week in 3N HCl, and at least 1 week in 2N HNO₃) low-density polyethylene bottles. Samples were stored frozen and in the dark until analysis (~ 1 week later in 2003 and 7 weeks later in 2004).

2.2. Aerosol Collection

[8] Aerosol samples were collected using a Total Suspended Particle (TSP) High Volume Sampler (HVS) placed on a roof at the Interuniversity Institute of Marine Sciences (IIMS) in Eilat, a few meters off the northwest coast of the Gulf of Aqaba (29.52°N , 34.92°E). The HVS is designed to have four filter cartridges connected to separate flowmeters

thus collecting four filter samples simultaneously. The airflow path of the HVS and filter holders are made of all plastic to minimize contamination with respect to the measurement of trace metals. Samples were taken at least once a week over a 24 hour period with an air flow of $2.4\text{--}2.7\ \text{m}^3\ \text{h}^{-1}$ between 20 August 2003 and 21 November 2004. Total suspended particles are collected on preweighed acid washed 47-mm polycarbonate membrane filters. The filters are weighted again after collection and stored frozen in polystyrene Petri dishes inside plastic bags until further analysis.

[9] Aerosol concentrations were converted to fluxes by calculating a dry deposition velocity for each sampling date using a particle deposition model based on measured particle size distributions and local meteorological conditions. See Y. Chen *et al.* (Estimates of atmospheric dry deposition and associated input of nutrients to Gulf of Aqaba seawater, submitted to *Journal of Geophysical Research*, 2006) (hereinafter referred to as Chen *et al.*, submitted manuscript, 2006) for details.

2.3. Analytical Methods

[10] Samples for iron were thawed at room temperature and acidified with 4 mL 6N ultrapure HCl per L, 12–14 hours prior to analysis. Iron (III) was determined by flow injection analysis with chemiluminescence detection [Johnson *et al.*, 2003; Obata *et al.*, 1993]. The method was modified to include inline buffering of the sample to pH 3.3 with sodium acetate buffer just prior to loading onto the column. The blank associated with this step and with sample acidification was determined by analyzing acidified ultra-pure water ($18.2\ \text{M}\Omega$). The precision of the measurement was $\sim 10\%$ based on repeated measurement of a single sample on different days. The accuracy of the method was assessed by analyzing standard reference seawater (NASS-5, National Research Council, Canada); a value of $3.8 \pm 0.3\ \text{nmol L}^{-1}$ was determined, compared to the certified value of $3.7 \pm 0.6\ \text{nmol L}^{-1}$. We were concerned that Fe(III) in the samples may have been reduced to Fe(II) during the 14-hour acidification and subsequently not adsorbed to the 8-hydroxyquinoline column [Lohan *et al.*, 2005]. We therefore tested 10 samples by analyzing them before and 30 min after adding $10\ \mu\text{M H}_2\text{O}_2$. As there was no trend toward higher values after H₂O₂ addition, we concluded that 14 hours was not long enough to produce iron reduction in these samples, and therefore did not add H₂O₂ to the remaining samples.

[11] One aerosol filter for each sampling period was used for bulk digestion and total iron analysis. A strong-acid (HF-HNO₃) microwave digestion procedure in Teflon bombs was used following Chen and Siefert [2004]. Samples were digested along with blanks and standards and the atmospheric concentrations were then calculated using the mass of the extraction solution, the concentration of the element and the volume of the air sampled. Iron concentrations were determined by Inductively Coupled Plasma Optical Emission Spectroscopy (ICP-OES) in a matrix of 2% HNO₃.

[12] Samples for nutrient analysis were collected concurrently with iron samples and filtered through $0.45\text{-}\mu\text{m}$

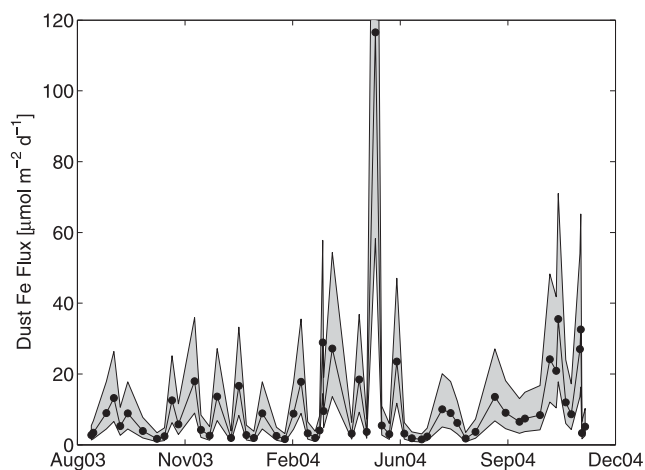


Figure 1. Estimated total flux of aerosol iron to the northern Gulf of Aqaba, August 2003 to November 2004. Aerosol samples were collected from a trace-metal clean aerosol sampler on the roof of the Steinitz Marine Science Center near Eilat, Israel. Iron concentrations were converted to fluxes using dry deposition velocities calculated from a particle deposition model (see Chen et al., submitted manuscript, 2006). The data points are enclosed in an envelope encompassing a twofold uncertainty in deposition velocity.

filters. Nitrite, nitrate and soluble reactive phosphorus (SRP) were analyzed using colorimetric methods described by *Grasshoff et al.* [1999], and modified for a Flow Injection Autoanalyzer (FIA, Lachat Instruments Model QuickChem 8000). SRP was preconcentrated by a factor of about 20 using the magnesium coprecipitation (MAGIC) method [*Karl and Tien*, 1992], followed by measurement using the FIA. The FIA was fully automated and peak areas were calibrated using standards prepared in low nutrient filtered seawater over a range of 0–10 $\mu\text{mol L}^{-1}$. The precision of these methods is 0.05 $\mu\text{mol L}^{-1}$ for NO_2 and NO_3 , and 0.01 $\mu\text{mol L}^{-1}$ for SRP.

3. Results

[13] Atmospheric iron deposition rates varied between 1.5 and 116 $\mu\text{mol m}^{-2} \text{d}^{-1}$, with a mean (September 2003 to September 2004) of 10 $\mu\text{mol m}^{-2} \text{d}^{-1}$. Total iron content of the aerosol varied between 0.5 and 6.7%, with a mean of 1.9%. Water soluble iron concentrations ranged between 0.06 and 1 nmol m^{-3} with a mean value of 0.5 nmol m^{-3} corresponding to 2–54 nmol mg^{-1} of aerosol sample [*Chen et al.*, 2006]. Iron fluxes showed considerable short-term variability about the mean (Figure 1). A single anomalously large (6 times the standard deviation) flux was measured on 10 May 2004. We believe this sample is in fact representative of a large flux event, and is not a methodological artifact, for three reasons. (1) Aerosol optical depth (AOD) data from SeaWiFS and MODIS between 1999 and 2004 shows a slight peak in AOD in the second quarter (April, May, June): The average AOD for the entire 6-year period is

0.134; the average second quarter AOD is 0.153. There are no valid MODIS or SeaWiFS satellite data available for the Gulf of Aqaba on 10 May 2004, but the MODIS record shows another very high dust day later that month, and the 2003 record for both satellites shows multiple high dust events in the spring and summer months (R. Labiosa, personal communication, 2005). (2) The total aerosol mass measured on that day was more than 3 times greater than the next highest day, ruling out iron contamination. (3) Observations at the IIMS indicate there was a pronounced “haze” visible during the whole week of 10 May 2004 (A. Post, personal communication, 2004).

[14] The concentration of dissolved iron in surface waters varied between 5.2 and 13.0 nmol L^{-1} , with a mean of 8.8 nmol L^{-1} , in August 2003, and between 0.7 and 6.8 nmol L^{-1} with a mean of 1.8 nmol L^{-1} in March 2004 (Figure 2). Surface dissolvable iron concentrations were significantly higher, between 10.3 and 48.1 nmol L^{-1} , with a mean of 21.8 nmol L^{-1} , in August, and between 1.9 and 43.7 nmol L^{-1} , with a mean of 6.7 nmol L^{-1} , in March (Figure 2).

[15] Profiles at Station A (29.46°N, 34.93°E, 700 m deep) in the north central Gulf (see Figure 2) show large differences in vertical structure between August and March (Figure 3). In August, the water column is thermally stratified, with a mixed layer of ~ 20 m. During winter, and into March, the water column is deeply mixed, in 2004 to a depth of ~ 450 m. In August, both dissolved and total iron show a pronounced surface maximum, approaching minimum and constant values of ~ 1 nmol L^{-1} (dissolved) and 4 nmol L^{-1} (total) below 40 m (Figure 3). In March, dissolved iron concentrations are about 1 nmol L^{-1} throughout the water column, and total iron, though more variable, is between 3–7.5 nmol L^{-1} with no surface maximum. Macronutrient concentrations show roughly the opposite trend, with low surface concentrations, near the detection limit, (0.15 $\mu\text{mol L}^{-1}$ nitrate + nitrite) observed in August, and higher concentrations in March (1.2 $\mu\text{mol L}^{-1}$) (Figure 3). Similar results are seen for SRP (0.03 and 0.07 $\mu\text{mol L}^{-1}$ in August and March, respectively) and Si (1.0 and 1.1 $\mu\text{mol L}^{-1}$ in August and March, respectively) in surface waters. In both August and March, macronutrient concentrations increase below the mixed layer, whereas iron concentrations do not. In August, nitrate is uniformly low to almost 100 m below the base of the mixed layer.

4. Discussion

[16] Converting measured metal concentrations in air to fluxes to the sea surface involves estimating the rate of iron-bearing particle deposition. We use a particle size dependent deposition model to estimate this velocity and assume that iron is uniformly distributed among different aerosol sizes (size fractionated iron concentrations are not available). Iron, however, generally occurs in the coarse ($>5 \mu\text{m}$) aerosol fraction [*Duce et al.*, 1991] and the coarse particles make up about 60% of the particle volume at our site. These coarse particles largely determine the total dry deposition velocity (Chen et al., submitted manuscript, 2006). Accord-

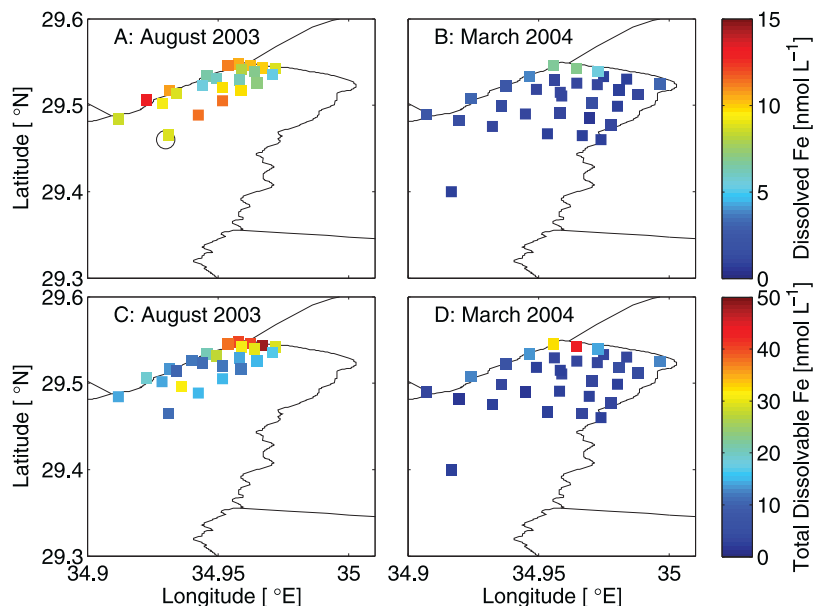


Figure 2. Concentration of dissolved and total dissolvable iron in the surface waters of the northern Gulf of Aqaba in August 2003 and March 2004. The location of Station A is indicated by the open circle in Figure 2a.

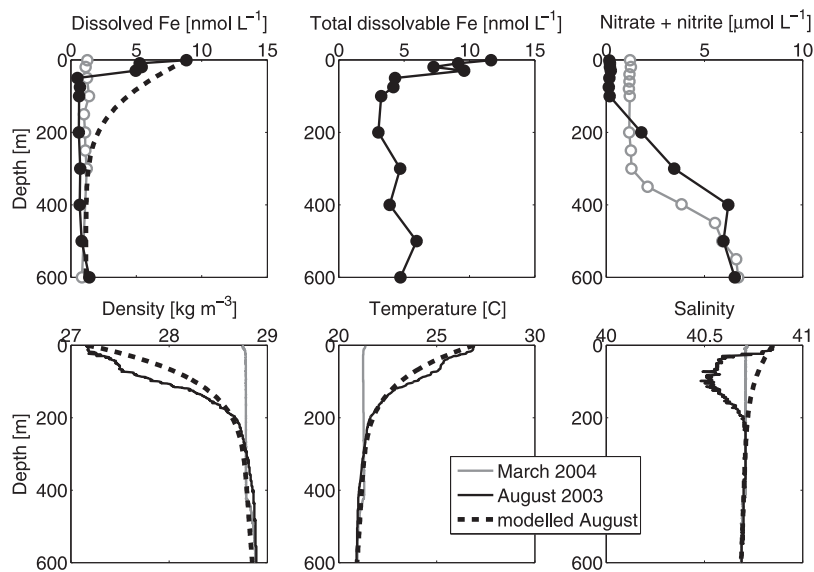


Figure 3. Profiles of dissolved Fe, total dissolvable Fe, nitrate, density, temperature, and salinity in August 2003 and March 2004 at Station A (29.46°N, 34.93°E) in the Gulf of Aqaba. Also shown are results from a one-dimensional model initialized in March and run until August. In this run, which includes complexation by an organic ligand present at a constant concentration of 0.6 nM with a conditional stability constant of $1.2 \times 10^{13} \text{ M}^{-1}$ [Archer and Johnson, 2000], the scavenging rate for dissolved iron, K_{Fe} , was constant with depth and equal to 0.01 yr^{-1} and the fraction of aerosol iron solubilized in the surface was 2%. The time-varying iron input time series was used to force the model. See text for details.

ingly, our calculated iron fluxes are relatively insensitive to the assumption of uniform distribution.

[17] Our estimates of atmospheric iron deposition rate in the Gulf of Aqaba confirm that this is indeed a region with an exceptionally large input of iron from dust. The total dust deposition rate, $28 \text{ g m}^{-2} \text{ yr}^{-1}$, agrees well with the value for this region predicted by a recent compilation of three observation-based models ($10\text{--}20 \text{ g m}^{-2} \text{ yr}^{-1}$) [Jickells *et al.*, 2005], making it one of the highest dust deposition rate areas on Earth. The annual iron deposition rate, $10 \mu\text{mol m}^{-2} \text{ d}^{-1}$, is about 4 times greater than the annual iron input rate to the Sargasso Sea [Jickells, 1999], and about 10 times greater than that to the Hawaiian island of Oahu [Prospero *et al.*, 1989].

[18] Our measurements of dissolved iron in the Gulf waters confirm our initial hypothesis that iron concentrations would be high and nonlimiting. Indeed, in both August and March, mixed layer dissolved iron concentrations were in excess of 1 nmol L^{-1} , significantly higher than the half saturation constant for growth with respect to iron [Blain *et al.*, 2002; Coale *et al.*, 2003]. In contrast, soluble reactive phosphorus and dissolved inorganic nitrogen concentrations in August in the surface layer are $2\text{--}40 \text{ nmol L}^{-1}$ and $40\text{--}75 \text{ nmol L}^{-1}$, respectively, potentially low enough for single limitation by either macro nutrient or colimitation [Thingstad *et al.*, 2005; Zohary and Robarts, 1998].

[19] These dissolved iron concentrations are higher than the theoretical solubility limit for iron in seawater ($\sim 0.08 \pm 0.03 \text{ nmol L}^{-1}$ [Millero, 1998; Wu *et al.*, 2001]). Such supersaturated iron concentrations in the $<0.2\text{-}\mu\text{m}$ fraction could be maintained either by the presence of colloidal iron or through complexation by organic ligands. Alternatively, iron may be rapidly released from particles (by thermal dissolution or photochemistry) and then scavenged toward a solubility limit. It is of course possible that despite the high concentration of dissolved iron, concentrations of biologically available iron are low. However, we conducted trace-metal clean incubation experiments in November 2004 and did not find enhanced growth when iron was added, indicating that ambient dissolved iron concentrations are not limiting (Z. Chase, unpublished data, 2004).

[20] The dissolved iron concentrations observed in surface waters of the Gulf of Aqaba are significantly higher than seen in the open ocean globally [Johnson *et al.*, 1997]. However, our August and March data are lower than previously reported for surface waters of the northern Gulf of Aqaba (15.6 nmol L^{-1}) and the northern Red Sea ($15\text{--}23 \text{ nmol L}^{-1}$) for samples collected in February 1999 [Shriadah *et al.*, 2004]. Our surface water dissolved iron concentrations in August are similar to what was observed in October in the Mediterranean, a nearby semienclosed basin, while concentrations in March are higher than the $<0.13 \text{ nmol L}^{-1}$ observed in the Mediterranean in February [Sarhou and Jeandel, 2001]. Our March surface water concentrations are similar to those observed in the Arabian Sea in January and April (mean 1.0 nmol L^{-1}), but the high concentrations we observed in August were not observed in the Arabian Sea, even after the SW Monsoon [Measures and Vink, 1999].

[21] Although dissolved iron concentrations are high throughout the year we observed substantial spatial variability in surface water concentrations (Figure 2). It is not clear what is driving the spatial variability in iron concentrations in the Gulf, which is most pronounced for total dissolvable iron. Specifically, very high concentrations of total dissolvable iron were measured at the northern-most stations, on the Israeli side of the Gulf (Figure 2). These sites are adjacent to the commercial center of the town of Eilat, as well as a fish farm operation. These are both potential sources of particulate iron. Another possibility is that there is a strong gradient in aeolian iron supply. The predominant wind direction is from the north, and some large mineral particles may be blown from the land immediately to the north, and deposited on the ocean within a short distance. Finally, there may be a benthic source of iron at these sites, as they are shallow sites where the bottom is sand, and not coral.

[22] In addition to spatial variability, there are marked seasonal differences in the distribution of dissolved and total iron in the northern Gulf of Aqaba, with high surface concentrations in August and lower, more uniform concentrations in March. A similar seasonal cycle has been observed in the Mediterranean [Sarhou and Jeandel, 2001]. The higher surface water iron concentrations observed in August cannot be due to greater dust input at that time; there is no significant seasonal trend in aerosol loads in Eilat, and in both 2004 and 2005 anomalously large aerosol loadings (threefold greater than average) were observed in spring (May and April, respectively, Figure 1 and Chen *et al.* (submitted manuscript, 2006)). We suggest the higher surface concentrations in August are due to (1) shoaling of the mixed layer and (2) limited biological iron removal due to macronutrients-limited productivity. That is, iron is able to accumulate throughout the summer in a shallow, isolated surface layer, with minimal removal by biological production.

4.1. A Simple Model

[23] We have used a simple one dimensional model to quantify what we know about the behavior of iron in this system. We assume that the only input of iron to the system is from aerosols in the form of dry deposition. Precipitation is virtually nonexistent in the summer as typically there is no rainfall between April and September in Eilat (average rainfall, occurring mainly in the winter, is only 3 cm yr^{-1} [Morcos, 1970]). Likewise there is practically no runoff. The fact that the Gulf is a rift valley, with very steep sides and a sandy bottom suggests inputs of iron from benthic sources will be minimal. Although this has not been confirmed directly, several lines of evidence suggest benthic sources are indeed minimal. First, profiles even within 1 km of the shore consistently show a surface and not a near-bottom maximum in iron. This is in contrast to the California [Chase *et al.*, 2005b] and Oregon [Chase *et al.*, 2005a, 2002] margins, where benthic sources are significant, and profiles consistently show a near-bottom maximum in iron concentration. Second, elevated concentrations are found at the most shoreward sites, but beyond that, concentrations are very uniform and there is little evidence of a gradient in iron concentration from the margins to the

center of the Gulf (e.g., Figure 2). As discussed above, there is some suggestion of a north to south gradient in iron at the northern end of the Gulf (Figure 2), but not an east-west gradient, suggesting the N-S gradient is related to local anthropogenic inputs from the cities of Eilat and Aqaba. We further assume no advective inputs or losses of iron. One of the outcomes of the modeling exercise is to show that this assumption is probably not valid.

[24] Because we are using data from August 2003 and March 2004, in order to calculate a seasonal change we need to assume that these months are representative of the respective seasons and that there is no interannual variability in the atmospheric iron flux. An analysis of MODIS and SeaWiFS aerosol optical depth data from 1999–2004 found interannual variability in summer values to be less than 10% (R. Labiosa, personal communication, 2005). Aerosol concentrations have been measured and fluxes estimated in Eilat for two summer seasons, 2004 and 2005 (Chen et al., submitted manuscript, 2006). The two years were very similar in terms of mean March–August aerosol flux (34 and 36 mg m⁻² d⁻¹ in 2004 and 2005, respectively) as well as the minimum (8 and 9 mg m⁻² d⁻¹) and maximum (264 and 230 mg m⁻² d⁻¹) recorded fluxes. Furthermore, in both years there was one high flux event significantly above the average; in 2004 it was on 10 May, and in 2005, 7 April. Finally, we have compared the March through September results of the real-time Navy Aerosol Analysis and Prediction System (NAAPS) for 2003 and 2004 (Naval Research Laboratory, Aerosol plot generator, 2004, <http://www.nrlmry.navy.mil/flambe/plotgen/index.htm>). Both years have almost the same average aerosol optical depth over this period (0.26 and 0.29 in 2003 and 2004, respectively). In summary, although a longer aerosol time series and/or coincident aerosol and ocean sampling is certainly preferable, from the above considerations we expect iron aerosol fluxes are relatively stable year to year in this region.

[25] With these assumptions, our hypothesis is that the summertime progression of dissolved iron concentrations in the Gulf of Aqaba can be explained as the balance between aerosol input and dissolution, vertical mixing, abiotic scavenging and biological uptake as presented by equations (1)–(5),

$$\frac{dFe(z)}{dt} = \frac{\partial}{\partial z} K_v \frac{\partial Fe(z)}{\partial z} + J_T(z)\alpha - Q \times P(z) \times e - K_{Fe}[Fe'(z)] \quad (1)$$

where

$$\frac{\partial}{\partial z} K_v \frac{\partial Fe(0)}{\partial z} = 0, \quad (2)$$

$$J_T(0) = 13 \mu\text{mol m}^{-2}\text{d}^{-1} \text{ or } = f(\text{time}), \quad (3)$$

$$\frac{\partial}{\partial z} K_v \frac{\partial Fe(600)}{\partial z} = 0, \quad (4)$$

$$J_T(z \neq 0) = 0. \quad (5)$$

[26] The first term on the right-hand side of equation (1) represents vertical diffusivity, where K_v , the eddy diffusivity coefficient, was estimated to be 10⁻³ m² s⁻¹, on the basis of modeling the temperature profiles, as shown below. The next term is the product of total aerosol iron deposition (J_T) and iron aerosol solubility (α). We used two formulations for J_T . In one, a constant iron flux was applied between 1 March and 1 September, equal to the measured average flux over this period in 2004 (13 $\mu\text{mol m}^{-2} \text{d}^{-1}$). We also tested a formulation where the iron input varied as a function of time, based on the 2004 measurements (Figure 1). In the model all of the dissolution occurs within the surface layer (equations (3) and (5)). Aerosol solubility was treated as a free parameter. The next term represents iron loss through biological uptake, and is the product of the primary production (P), an average cellular Fe:C ratio (Q) and the ratio of export production to total production (e). Because we might expect Fe:C ratios to be elevated in this environment with high dissolved iron, we set Q equal to 20 $\mu\text{mol:mol}$, a value that has been observed in phytoplankton cultures supplied with abundant iron [Maldonado and Price, 1996; Sunda and Huntsman, 1995]. P was taken as the average summertime primary productivity in the Gulf (17 mmol C m⁻² d⁻¹; based on unpublished ¹⁴C incubation data from 1999–2002 (David Illuz, personal communication, 2004)). We have assumed a constant primary production rate in the upper 100 m, and zero productivity below this depth. In the absence of direct measurement of new and regenerated production in this system we used an upper limit of 0.3 for the ratio of export production to total production (e) in this warm oligotrophic system [Laws et al., 2000]. The last term in equation (1) represents loss due to abiotic scavenging, which is formulated two different ways after Archer and Johnson [2000]. In one formulation, we assume no complexation by an organic ligand, and scavenging is proportional to dissolved iron concentration ($Fe(z) = Fe'(z)$ in equation (1)). We also tested the formulation that includes complexation of iron by an organic ligand having a concentration of 0.6 nmol L⁻¹ and a conditional stability constant of 1.2 × 10¹³ M⁻¹. These parameter values were chosen to match those used by Archer and Johnson [2000]. In this case only the uncomplexed iron (Fe') is available to be scavenged. In both cases scavenging rate constants were varied tenfold around values optimized by Archer and Johnson [2000].

[27] The model is initialized with the March 2004 profiles. We modeled the temperature and salinity profiles using a similar approach by adding a heating (salt) term to the uppermost layer equivalent to the total heating (salinity increase) observed at the surface between March and August and mixing that input vertically by eddy diffusivity. The best fit to the temperature data was obtained with a K_v of 10⁻³ m² s⁻¹ (Figure 3). Lower values, such as the canonical 10⁻⁴ m² s⁻¹ [Munk, 1966] or the 10⁻⁵ m² s⁻¹ observed in deliberate trace experiments [Law et al., 2003], produce temperatures at depth that are significantly too low in August. K_v was also calculated from the vertical velocity field generated by a three-dimensional primitive equation model of the Gulf of Aqaba; over the whole summer, in the upper 200 m the value of K_v is 3.5 × 10⁻³

$\text{m}^2 \text{s}^{-1}$ (R. Labiosa, personal communication, 2005). A similar value of $2.5 \times 10^{-3} \text{ m}^2 \text{s}^{-1}$ was calculated on the basis of nitrate profiles and consideration of nitrate uptake kinetics [Badran *et al.*, 2005]. Convective mixing is also important in the Gulf. However, convective processes dominate during the winter season (December–April), whereas eddy diffusion dominates the mixing in the summer (May through November) [Badran *et al.*, 2005], which is what we are interested in modeling. The relatively large diffusion coefficient required in this model may result in part from the fact that we have not included convection; an earlier one-dimensional model reproduced temperature profiles throughout the year with a convective scheme forced by local meteorological conditions and much weaker diffusion ($K_v = 10^{-6} \text{ m}^2 \text{s}^{-1}$) [Wolf-Vecht *et al.*, 1992].

[28] The August salinity profile is not fit by a simple mixing model using $K_v = 10^{-3} \text{ m}^2 \text{s}^{-1}$; there is clearly an intrusion of lower-salinity water centered around 100 m (Figure 3). A salinity minimum at about 100 m is regularly observed during the summer in the northern Gulf of Aqaba [Wolf-Vecht *et al.*, 1992; A. Rivlin, personal communication, 2005]. As suggested by Wolf-Vecht *et al.* [1992] the only possible source of this low salinity water is from the Red Sea proper, across the Straights of Tiran.

[29] The model also does a poor job of reproducing dissolved iron concentrations beneath the surface in August. As we discuss in section 4.2, a solubility of 2% produces a good fit to the surface iron data in August using a variety of different model formulations. However, none of these formulations reproduces the profile below the surface (for example, see output in Figure 3). We believe the most likely explanation for this discrepancy is that there is an advective input of low iron water into the Gulf, associated with the clearly visible intrusion of lower salinity water at about 100 m. There are other possible explanations. First, iron loss terms may be elevated in the region of discrepancy, between 5 and 70 m. For example, if we increase the biological export term ($Q \times P \times e$) by a factor of 250–300 between 5 and 70 m the iron profile is reproduced reasonably well. However, such a large increase in biological removal of iron is difficult to justify, given an already generous choice of Q and e , unless productivity in this depth range was anomalously high in 2003. We need to increase the scavenging term a thousandfold, relative to the surface, between 30 and 70 m in order to reproduce the observed profile. Such an extreme increase in the scavenging term at this depth is difficult to justify. Second, if mixing is reduced by an order of magnitude, setting K_v to $10^{-4} \text{ m}^2 \text{s}^{-1}$, the iron distribution in August is well reproduced (with a slightly higher solubility of 2.5%), because the iron is retained in the surface layer. However, as explained above, with such slow mixing the sub-surface water column is too cold in August relative to observations. Finally, a large dust event just prior to our sampling in August 2003 (i.e., prior to the period of aerosol flux measurement) cannot account for the observed iron vertical profile, unless average fluxes the rest of the summer were anomalously low, because excess iron still accumulates throughout the summer. How-

ever, as discussed above, the NAAPS results suggest 2003 and 2004 had similar total summer aerosol loads, and a more detailed examination of the 2003 summer NAAPS model shows quite constant values, with one 4-sigma dust event in late May and nothing anomalous in August.

[30] We have not included a remineralization term in the model. Doing so, for example following the formulation of Johnson *et al.* [1997], based on carbon flux, has little impact on the outcome, and produces a worse fit to the data, since it acts as a subsurface iron source, when the model is lacking an iron sink.

[31] We have not attempted to model total dissolvable iron, because of the operational nature of the measurement and because we don't know the size distribution of total iron, which affects its sinking rate and the extent to which it acts like a solute or like a solid. Features such as the "spike" in dissolvable iron near 50 m in March (Figure 2) are difficult to account for in the simple model used to describe dissolved iron. Furthermore, there is clearly strong spatial variability in total dissolvable iron (Figure 2), which suggests there may be local sources of aerosol or nonaerosol particulate Fe. In principle, such sources could affect dissolved iron distributions as well through dissolution, and there is some indication of elevated concentrations of dissolved iron associated with elevated concentrations of dissolvable iron in surface waters (Figure 2). The dynamic range for dissolved iron is much smaller than for total iron, suggesting minimum impact of local sources on the dissolved iron distributions. Variable inputs (or outputs such as scavenging intensity) would need to be considered and quantified in a more complete model of iron cycling in the Gulf.

[32] In summary, we have used a simple model to represent a hypothesis about what controls the evolution of dissolved iron concentrations over the summer in the northern Gulf of Aqaba. This model, which includes only aerosol deposition, diffusive mixing and loss due to scavenging and biological uptake, can reproduce surface dissolved iron concentrations in August, but does a poor job of reproducing the dissolved iron profile beneath the surface. The most likely explanation is that iron concentrations within the Gulf are influenced, at least during the summer of 2003, by the advection of low-iron water at a depth of 30–70 m. While this simple model works reasonably well during the summer, a model of the entire annual cycle would need to account for convective mixing during the winter.

4.2. Iron Solubility and Residence Times

[33] One of the goals of the modeling exercise was to constrain the value of the solubility of aerosol iron, by determining which value gives the best fit to the data. Because the subsurface iron profile was not well fit by the model, we focus on the aerosol solubility necessary to account for the observed seasonal accumulation of iron in the surface layer. A solubility of 2% was found to produce the best fit, irrespective of the exact parameterization of iron scavenging, and across a range of reasonable values of the iron scavenging rate constant (Table 1). This result holds whether a constant summer iron flux or a time-varying

Table 1. Results of Model Runs Used to Determine the Best Fit for the Solubility of Dry Deposited Iron^a

Scavenging Rate, yr ⁻¹	Best Fit, Solubility, %	Best Fit, Model-Data, nM
<i>Constant Dust, No Ligand</i>		
0.00032	2	0.56
0.0016	2	0.53
0.008	2	0.40
0.016	5	12.39
<i>Variable Dust, No Ligand</i>		
0.00032	2	0.02
0.0016	2	-0.01
0.008	2	-0.17
0.016	5	10.91
<i>Constant Dust, Ligand</i>		
0.002	2	0.52
0.01	2	0.36
0.05	5	-0.38
0.01	5	12.66
<i>Variable Dust, Ligand</i>		
0.002	2	-0.02
0.01	2	-0.21
0.05	2.5	0.64
0.01	5	11.24

^aThe one-dimensional model was run in a configuration with no complexation by organic ligands, and in a configuration that included scavenging by an organic ligand having a concentration of 0.6 nmol L^{-1} and a conditional stability constant of 1.2×10^{13} . Both configurations were run with two different time series of iron inputs. In the “variable dust” run, iron inputs were based on the time series of measured aerosol load and estimated total iron flux in 2004. In the “constant dust” model, the same average flux as determined from 2004 measurements was used, but the flux was evenly distributed throughout the time period modeled. The solubility giving the best fit to surface dissolved iron data in August was determined for a range of values of the scavenging rate constant (midpoint values were those determined by Archer and Johnson [2000] as being the best fit to global iron measurements). The fit assuming the fraction of iron that dissolves is 5% is also indicated.

summer iron flux is used (Figure 4). A recent review of aerosol iron solubility [Jickells and Spokes, 2001] concluded that overall aerosol iron solubility is probably less than or equal to 2%, reflecting a large fraction of dry deposition with low solubility ($\sim 0.1\%$) and a lower fraction of wet deposition with high solubility ($\sim 5\%$). Our estimated total solubility is thus similar to recent estimates of overall iron solubility, but because the deposition is entirely dry in this region, it suggests the fraction of dry deposition that dissolves in this region is at the high end of previous estimates for other regions.

[34] Chen *et al.* [2006] have directly measured the solubility of iron in aerosol samples collected at our study site. Using a 30-min leach in filtered seawater with a particulate concentration of 60 mg L^{-1} in the leaching jar, they find on average 0.3% solubility for iron. While consistent with other laboratory estimates of aerosol solubility in seawater (as reviewed by Jickells and Spokes [2001]), such a low solubility is not consistent with the observed surface water enrichment in August. Total iron fluxes would have to be sixfold higher than estimated from measurements for the measured surface iron concentrations to be consistent with a solubility as low as 0.3%. The difference may reflect additional solubilization that occurs when aerosols reside

in the real surface ocean for an extended period of time. Alternatively, the low solubility measured experimentally may be due to the relatively high particulate concentration (60 mg L^{-1}) used. Bonnet and Guieu [2004] found an inverse power law relationship between the percent of iron dissolved from natural and anthropogenic aerosol samples over 7 days and the concentration of aerosol particles in the leaching jar, with greater iron solubility at lower particle concentrations. Applying this power law relationship to the experimental concentration of 60 mg L^{-1} used by Chen *et al.* [2006] predicts solubilities of 0.015% and 0.3% for natural and anthropogenic particles, respectively. The fact that the measured solubility at 60 mg L^{-1} shows better agreement with the anthropogenic than with the natural (Saharan) aerosol may reflect either a preponderance of anthropogenic aerosol in the Gulf of Aqaba, differences in the solubility of natural aerosol in these two regions, differences between a 30-min and a 7-day leach or the difference between a soil sample and an aerosol sample.

[35] Assuming 2% of the aerosol iron dissolves, we can divide the “annual” average iron inventory (Table 2) by the annual dissolved iron flux ($2\% \times$ total iron flux) to calculate the residence time of dissolved iron with respect to aerosol deposition. A similar calculation can be made for total iron, using the total iron flux. These estimates (Table 3) have uncertainty associated with estimating the annual inventory from two seasons, from the calculation of iron deposition

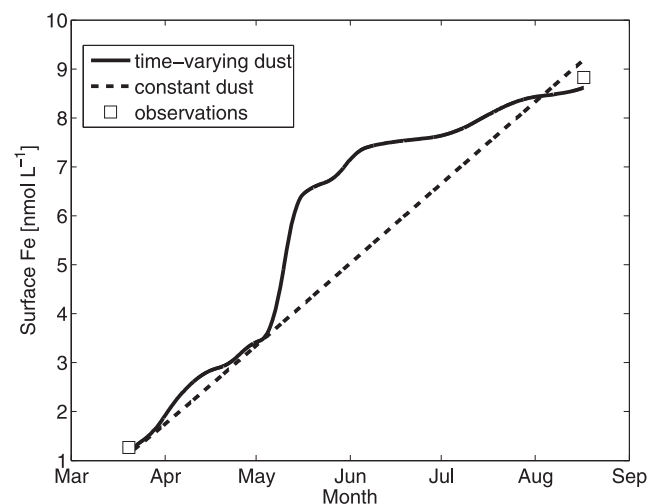


Figure 4. Time series of dissolved iron at 5m in the Gulf of Aqaba between 20 March and 20 August. Curves are the model-derived values using the “ligand” model, with an iron solubility of 2% and a scavenging rate of 0.01 yr^{-1} . In the “time-varying dust” run, iron inputs were based on the time series of measured aerosol load and estimated total iron flux in 2004. In the “constant dust” model, the same average flux as determined from 2004 measurements was used, but the flux was evenly distributed throughout the time period modeled. White squares represent measured concentrations in March 2004 and August 2003. The model was initiated with observed iron concentrations in March 2004.

Table 2. Vertically Integrated Inventory of Dissolved and Total Iron in March 2004 and August 2003, and an “Annual” Average Consisting of the March–August Average^a

Depth, m	March		August		“Annual” Average	
	Dissolved Inventory	Total Inventory	Dissolved Inventory	Total Inventory	Dissolved Inventory	Total Inventory
0–50	26 ± 5	99 ± 40	117 ± ...	200 ± ...	71 ± 46	149 ± 60
0–100	79 ± 10	305 ± 103	175 ± ...	392 ± ...	127 ± 56	349 ± 88
0–200	186 ± 9	659 ± 76	259 ± ...	723 ± ..	223 ± 43	691 ± 65
0–300	270 ± 38	917 ± 165	335 ± ...	1106 ± ...	302 ± 44	1011 ± 165
0–500	461 ± 83	1587 ± 341	486 ± ...	2012 ± ...	474 ± 61	1799 ± 344

^aUnits are $\mu\text{mol m}^{-2}$. In March, the average and 1 standard deviation from profiles at three different locations are indicated. A single profile from station A was used in August. Inventories were calculated by trapezoidal integration.

rate, and, for dissolved iron, from the estimated solubility. Such uncertainty is generally present in all estimates of iron residence time.

[36] We find a dissolved iron residence time of about half a year near the surface, which is far shorter than the residence time of iron in the ocean as a whole [Bruland *et al.*, 1994], but similar to a recent estimate of iron residence time in surface waters of the North Pacific [Boyle *et al.*, 2005]. Our results are also largely consistent with estimates of dissolved iron residence time in the upper 100 m of the Sargasso Sea, which Jickells [1999] estimated to be 253 days. Residence times for total iron are about tenfold shorter than for dissolved iron, varying from weeks at the surface to almost a year within the upper 500 m (Table 3). These short residence times are consistent with results from the Sargasso Sea (18 days in the upper 100 m [Jickells, 1999]) and from the equatorial Atlantic (6–62 days in the upper 200 m [Croot *et al.*, 2004]).

4.3. A Global Context

[37] The relationship between the local rate of aerosol deposition and the iron inventory in the underlying water column is of interest because it should give an indication of whether iron solubility limits the amount of dissolved iron that can accumulate in the water column. In their global compilation, Johnson *et al.* [1997] found a weak relationship between aeolian iron flux and the 0- to 500-m integrated dissolved iron inventory. The data could be fit

with either a linear or a power law relationship. These two equations make very different predictions about the integrated iron inventories expected at locations where the aeolian iron fluxes are greater than those included in the 1997 data set. The annual aeolian iron flux in the Gulf of Aqaba is almost 2 orders of magnitude greater than the greatest flux in the Johnson *et al.* [1997] compilation. Plotting the Gulf of Aqaba annually averaged data together with the two curves fit to the Johnson *et al.* [1997] data shows clearly that the new data agree better with the power law than with the linear relationship (Figure 5). This asymptotic relationship implies that there is a solu-

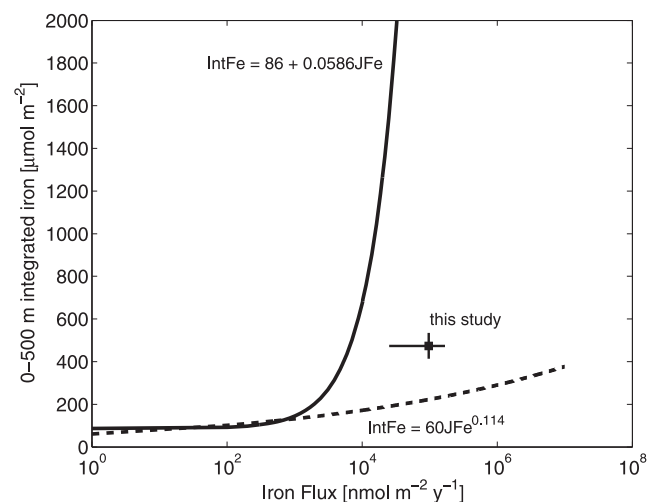


Figure 5. Relationship between the atmospheric deposition of dissolved iron to the sea surface and the dissolved iron concentration integrated from the surface to 500 m. The two curves are fits to the data compiled by Johnson *et al.* [1997]. See that reference for details of the data used in the compilation. The square shows the data for the Gulf of Aqaba. The range of iron flux represents the September 2003 to September 2004 measured iron input from dust multiplied by a fraction from 1 to 3% to account for dissolution, and including a twofold uncertainty in depositional velocity. The integrated iron inventory is the average of inventories for August 2003 and March 2004 and the range is the associated standard deviation (Table 1).

Table 3. Residence Time of Total Iron and Dissolved Iron in the Gulf of Aqaba With Respect to Aerosol Deposition, as a Function of Integration Depth^a

Depth, m	Residence Time	
	Total Iron, days	Dissolved Iron, years
0–50	7.4–29.4	0.4–1.5
0–100	17.2–68.7	0.7–2.7
0–200	34.0–136.1	1.2–4.8
0–300	49.8–199.3	1.6–6.5
0–500	88.6–354.6	2.6–10.2

^aAnnual average inventories were divided by estimated annual iron input from dust. A solubility of 2% was used in estimating the input of dissolved iron. The range of values reflects an estimated twofold uncertainty in deposition velocity.

bility control on dissolved iron concentrations. As aeolian input increases, the amount of dissolved iron in the water column does not increase continuously, but rather approaches a limit dictated by the solubility of iron in seawater.

[38] **Acknowledgments.** We thank Anton Post, Gregory Cutter, and Sergio Sañudo-Wilhelmy for the use of equipment and laboratory facilities, Rochelle Labiosa and Jonathan Nash for discussion, and Asaph Rivlin, Rochelle Labiosa, Megan Young, and Michael Calhoun for assistance in the field. Funding for this work was provided by the NASA New Investigator Program NAG5-12663 to A. P.

References

- Archer, D. E., and K. Johnson (2000), A model of the iron cycle in the ocean, *Global Biogeochem. Cycles*, *14*, 269–279.
- Badran, M. I., M. Rasheed, R. Manasrah, and T. Al-Najjar (2005), Nutrient flux fuels the summer primary productivity in the oligotrophic waters of the Gulf of Aqaba, Red Sea, *Oceanologia*, *47*, 47–60.
- Blain, S., P. N. Sedwick, F. B. Griffiths, B. Queguiner, E. Bucciarelli, M. Fiala, P. Pondaven, and P. Treguer (2002), Quantification of algal iron requirements in the Subantarctic Southern Ocean (Indian sector), *Deep Sea Res., Part II*, *49*, 3255–3273.
- Bonnet, S., and C. Guieu (2004), Dissolution of atmospheric iron in seawater, *Geophys. Res. Lett.*, *31*, L03303, doi:10.1029/2003GL018423.
- Boyle, E. A., B. A. Bergquist, R. A. Kayser, and N. Mahowald (2005), Iron, manganese, and lead at Hawaii Ocean Time-series station ALOHA: Temporal variability and an intermediate water hydrothermal plume, *Geochim. Cosmochim. Acta*, *69*, 933–952.
- Bruland, K. W., K. J. Orians, and J. P. Cowen (1994), Reactive trace metals in the stratified central North Pacific, *Geochim. Cosmochim. Acta*, *58*, 3171–3182.
- Chase, Z., A. van Geen, M. P. Kosro, J. Marra, and P. A. Wheeler (2002), Iron, nutrient and phytoplankton distributions in Oregon coastal waters, *J. Geophys. Res.*, *107*(C10), 3174, doi:10.1029/2001JC000987.
- Chase, Z., B. Hales, T. J. Cowles, R. Schwartz, and A. van Geen (2005a), Distribution and variability of iron input to Oregon coastal waters during the upwelling season, *J. Geophys. Res.*, *110*, C10S12, doi:10.1029/2004JC002590.
- Chase, Z., K. S. Johnson, V. A. Elrod, J. N. Plant, S. E. Fitzwater, L. Pickell, and C. M. Sakamoto (2005b), Manganese and iron distributions off central California influenced by upwelling and shelf width, *Mar. Chem.*, *95*, 235–254.
- Chen, Y., and R. L. Siefert (2004), Seasonal and spatial distributions and dry deposition fluxes of atmospheric total and labile iron over the tropical and subtropical North Atlantic Ocean., *J. Geophys. Res.*, *109*, D09305, doi:10.1029/2003JD003958.
- Chen, Y., J. Street, and A. Paytan (2006), Comparison between pure-water- and seawater-soluble nutrient concentrations of aerosols from the Gulf of Aqaba, *Mar. Chem.*, *101*(1–2), 141, doi:10.1016/j.marchem.2006.02.002.
- Coale, K. H., X. Wang, S. J. Tanner, and K. S. Johnson (2003), Phytoplankton growth and biological response to iron and zinc additions in the Ross Sea and Antarctic Circumpolar Current along 170°W, *Deep Sea Res., Part II*, *50*, 635–653.
- Croot, P. L., P. Streu, and A. R. Baker (2004), Short residence time for iron in surface seawater impacted by atmospheric dry deposition from Saharan dust events, *Geophys. Res. Lett.*, *31*, L23S08, doi:10.1029/2004GL020153.
- Duce, R. A., and N. W. Tindale (1991), Atmospheric transport of iron and its deposition in the ocean, *Limnol. Oceanogr.*, *36*, 1715–1726.
- Duce, R. A., et al. (1991), The atmospheric input of trace species to the world ocean, *Global Biogeochem. Cycles*, *5*, 193–259.
- Fung, I. Y., S. K. Meyn, I. Tegen, S. C. Doney, J. G. John, and J. K. B. Bishop (2000), Iron supply and demand in the upper ocean, *Global Biogeochem. Cycles*, *14*, 281–295.
- Gao, Y., S.-M. Fan, and J. L. Sarmiento (2003), Aeolian iron input to the ocean through precipitation scavenging: A modeling perspective and its implications for natural iron fertilization in the ocean, *J. Geophys. Res.*, *108*(D7), 4221, doi:10.1029/2002JD002420.
- Genin, A., B. Lazar, and S. Brenner (1995), Vertical mixing and coral death in the Red Sea following the eruption of Mount Pinatubo, *Nature*, *377*, 507–510.
- Grasshoff, K., K. Kremling, and M. Ehrhardt (1999), *Methods of Seawater Analysis*, John Wiley, Hoboken, N. J.
- Jickells, T. D. (1999), The inputs of dust derived elements to the Sargasso Sea: A synthesis, *Mar. Chem.*, *68*, 5–14.
- Jickells, T. D., and L. J. Spokes (2001), Atmospheric iron inputs to the oceans, in *The Biogeochemistry of Iron in Seawater*, edited by D. R. Turner and K. A. Hunter, pp. 85–121, John Wiley, Hoboken, N. J.
- Jickells, T. D., et al. (2005), Global iron connections between desert dust, ocean biogeochemistry, and climate, *Science*, *308*, 67–71.
- Johnson, K. S., R. M. Gordon, and K. H. Coale (1997), What controls dissolved iron concentrations in the world ocean?, *Mar. Chem.*, *57*, 137–161.
- Johnson, K. S., et al. (2003), Surface-ocean lower atmosphere interactions in the Northeast Pacific ocean gyre: Aerosols, iron and the ecosystem response, *Global Biogeochem. Cycles*, *17*(2), 1063, doi:10.1029/2002GB002004.
- Karl, D., and G. Tien (1992), MAGIC: A sensitive and precise method for measuring dissolved phosphorus in aquatic environments, *Limnol. Oceanogr.*, *37*, 105–116.
- Labiosa, R. G., K. R. Arrigo, A. Genin, S. G. Monismith, and G. van Dijken (2003), The interplay between upwelling and deep convective mixing in determining the seasonal phytoplankton dynamics in the Gulf of Aqaba: Evidence from SeaWiFS and MODIS, *Limnol. Oceanogr.*, *48*, 2355–2368.
- Law, C. S., E. R. Abraham, A. J. Watson, and M. I. Liddicoat (2003), Vertical eddy diffusion and nutrient supply to the surface mixed layer of the Antarctic Circumpolar Current, *J. Geophys. Res.*, *108*(C8), 3272, doi:10.1029/2002JC001604.
- Laws, E. A., P. G. Falkowski, W. O. Smith Jr., H. Ducklow, and J. J. McCarthy (2000), Temperature effects on export production in the open ocean, *Global Biogeochem. Cycles*, *14*, 1231–1246.
- Lindell, D., and A. F. Post (1995), Ultraphytoplankton succession is triggered by deep winter mixing in the Gulf of Aqaba (Eilat), Red Sea, *Limnol. Oceanogr.*, *40*, 1130–1141.
- Lohan, M. C., A. M. Aguilar-Islas, R. P. Franks, and K. W. Bruland (2005), Determination of iron and copper in seawater at pH 1.7 with a new commercially available chelating resin, NTA Superflow, *Anal. Chim. Acta*, *530*, 121–129.
- Maldonado, M. T., and N. M. Price (1996), Influence of N substrate on Fe requirements of marine centric diatoms, *Mar. Ecol. Prog. Ser.*, *141*, 161–172.
- Measures, C. I., and S. Vink (1999), Seasonal variations in the distribution of Fe and Al in the surface waters of the Arabian Sea, *Deep Sea Res., Part II*, *46*, 1597–1622.
- Millero, F. J. (1998), Solubility of Fe in seawater, *Earth Planet. Sci. Lett.*, *154*, 323–329.
- Moore, J. K., S. C. Doney, D. M. Glover, and I. Y. Fung (2002), Iron cycling and nutrient-limitation patterns in surface waters of the World Ocean, *Deep Sea Res., Part II*, *49*, 463–507.
- Morcos, S. A. (1970), Physical and chemical oceanography of the Red Sea, *Oceanogr. Mar. Biol. Annu. Rev.*, *8*, 73–202.
- Munk, W. H. (1966), Abyssal recipes, *Deep Sea Res.*, *13*, 707–713.
- Obata, H., H. Karanati, and E. Nakatana (1993), Automated determination of iron in seawater by chelating resin concentration and chemiluminescence detection, *Anal. Chem.*, *65*, 1524–1528.
- Post, A. F., Z. Dedej, R. Gottlieb, H. Li, D. N. Thomas, M. El-Absawi, A. El-Naggar, M. El-Gharabawi, and U. Sommer (2002), Spatial and temporal distribution of Trichodesmium spp. in the stratified Gulf of Aqaba, Red Sea, *Mar. Ecol. Prog. Ser.*, *239*, 241–250.
- Prospero, J. M., M. Uematsu, and D. L. Savoie (1989), Mineral aerosol transport to the Pacific Ocean, in *Chemical Oceanography*, edited by J. P. Riley, Elsevier, New York.
- Sarthou, G., and C. Jeandel (2001), Seasonal variations of iron concentrations in the Ligurian Sea and iron budget in the western Mediterranean Sea, *Mar. Chem.*, *74*, 115–129.
- Shriadah, M. A., M. A. Okbah, and M. S. El-Deek (2004), Trace metals in the water columns of the Red Sea and the Gulf of Aqaba, Egypt, *Water Air Soil Pollut.*, *153*, 115–124.
- Sunda, W. G., and S. A. Huntsman (1995), Iron uptake and growth limitation in oceanic and coastal phytoplankton, *Mar. Chem.*, *50*, 189–206.
- Thingstad, T. F., et al. (2005), Nature of phosphorus limitation in the ultraoligotrophic eastern Mediterranean, *Science*, *309*, 1068–1071.
- Wolf-Vecht, A., N. Paldor, and S. Brenner (1992), Hydrographic indications of advection/convection effects in the Gulf of Elat, *Deep Sea Res., Part I*, *39*, 1393.
- Wu, J., W. Sunda, E. A. Boyle, and D. M. Karl (2000), Phosphate depletion in the western North Atlantic Ocean, *Science*, *289*, 759–762.
- Wu, J., E. A. Boyle, W. Sunda, and L.-S. Wen (2001), Soluble and colloidal iron in the oligotrophic North Atlantic and North Pacific, *Science*, *293*, 847–849.

Zohary, T., and D. R. Roberts (1998), Experimental study of microbial P limitation in the eastern Mediterranean, *Limnol. Oceanogr.*, *43*, 387–395.

Z. Chase, College of Oceanic and Atmospheric Sciences, Oregon State University, Ocean Administration Building 104, Corvallis, OR 97331-5503, USA. (zanna@coas.oregonstate.edu)

Y. Chen, A. Paytan, and J. Street, Department of Geological and Environmental Sciences, Stanford University, Building 320, Stanford, CA 94305, USA. (ychen04@stanford.edu; apaytan@pangea.stanford.edu; jstreet@stanford.edu)

K. S. Johnson, Monterey Bay Aquarium Research Institute, 7700 Sandholdt Road, Moss Landing, CA 95039, USA. (kjohnson@mbari.org)